J|A|C|S ARTICLES

Published on Web 10/29/2009

Preferential Interactions of Guanidinum Ions with Aromatic Groups over Aliphatic Groups

Philip E. Mason,[†] Christopher E. Dempsey,[‡] George W. Neilson,[§] Steve R. Kline,[||] and John W. Brady*,[†]

Department of Food Science, Cornell University, Ithaca, New York 14853, Department of Biochemistry, Bristol University, Bristol BS8 1TD, United Kingdom, H. H. Wills Physics Laboratory, Bristol University, Bristol BS8 1TL, United Kingdom, and Center for Neutron Research, National Institute of Standards and Technology, 100 Bureau Drive, Mail Stop 6102, Gaithersburg, Maryland 20899

Received April 29, 2009; E-mail: jwb7@cornell.edu

Abstract: Small angle neutron scattering (SANS) and molecular dynamics (MD) simulations were used to characterize the long-range structuring (aggregation) of aqueous solutions of isopropanol (IPA) and pyridine and the effect on structuring of guanidinium chloride (GdmCl). These solutes serve as highly soluble analogs of the nonpolar aliphatic (IPA) and aromatic (pyridine) side chains of proteins. SANS data showed that isopropanol and pyridine both form clusters in water resulting from interaction between nonpolar groups of the solutes, with pyridine aggregation producing longer-range structuring than isopropanol in 3 *m* solutions. Addition of GdmCl at 3 *m* concentration considerably reduced pyridine aggregation but had no effect on isopropanol aggregation. MD simulations of these solutions support the conclusion that long-range structuring involves hydrophobic solute interactions and that Gdm^+ interacts with the planar pyridine group to suppress pyridine−pyridine interactions in solution. Hydrophobic interactions involving the aliphatic groups of isopropanol were unaffected by GdmCl, indicating that the planar and weakly hydrated Gdm^+ cation cannot make productive interactions with the highly curved or "lumpy" aliphatic groups of this solute. These observations support the conclusion that the effects of Gdm^+ ions on protein-stabilizing interactions involving aromatic amino acid side chains make significant contributions to the denaturant activity of GdmCl, whereas interactions with the "lumpy" aliphatic side chains are likely to be less important.

Introduction

The mechanisms by which denaturants destabilize the folded structures of proteins relative to their unfolded states have been pursued for many decades.[1−4] Over a century ago, Hofmeister ranked cosolutes in the order of their effectiveness at salting proteins out of solution,[5] and this ranking was later found to be inversely correlated with the protein-denaturing activity of the solutes.[6] Recent studies indicate that this ranking correlates in part with the extent to which the solute is either concentrated at protein surfaces (for denaturants like urea and guanidinium, Gdm^+) or excluded from them (for conformation-stabilizing solutes like trimethylamine-*N*-oxide, trehalose, and sulfate).[7−11] In this mechanism, unfolding of the protein reveals additional surface for denaturant interactions, promoting the transition to unfolded states. Conformation-stabilizing solutes are excluded from the protein surface, which remains compact to limit interactions with solvent. The molecular basis of these effects often correlates with the hydration properties of the solutes, with weakly solvated species (denaturants) readily shedding hydration waters to interact with weakly solvated protein groups,[6,7,10,12,13] while more strongly hydrated species preferentially retain their hydration waters in the presence of a protein surface, raising the surface tension of the solution.[6,9,14] (The denaturant urea does not readily fit into this picture, however, since it is not weakly hydrated and can favorably interact with both polar and nonpolar groups.[15,16])

[†] Cornell University.
[‡] Department of Biochemistry, Bristol University.
[§] H. H. Wills Physics Laboratory, Bristol University.
[||] National Institute of Standards and Technology.

(1) Tanford, C. *Adv. Protein Chem.* **1968**, *23*, 121–282.
(2) Pace, C. N. *Methods Enzymol.* **1986**, *131*, 266–280.
(3) Makhatadze, G. I.; Privalov, P. L. *J. Mol. Biol.* **1992**, *226*, 491–505.
(4) Myers, J. K.; Pace, C. N.; Scholtz, J. M. *J. Protein Sci.* **1995**, *4*, 2138–2148.
(5) Hofmeister, F. *Naunyn-Schmiedeberg's Arch. Pharmacol.* **1888**, *24*, 247–260.
(6) Arakawa, T.; Timasheff, S. N. *Biochemistry* **1984**, *23*, 5912–5923.
(7) Lee, J. C.; Timasheff, S. N. *Biochemistry* **1974**, *13*, 257–265.
(8) Arakawa, T.; Timasheff, S. N. *Biochemistry* **1984**, *23*, 5924–5929.
(9) Collins, K. D. *Q. Rev. Biophys.* **1985**, *18*, 323–422.
(10) Courtenay, E. S.; Capp, M. W.; Record, M. T. *Protein Sci.* **2001**, *10*, 2485–2497.
(11) Street, T. O.; Bolen, D. W.; Rose, G. D. *Proc. Natl. Acad. Sci. U.S.A.* **2006**, *103*, 13997–14002.
(12) Collins, K. D. *Proc. Natl. Acad. Sci. U.S.A.* **1995**, *92*, 5553–5557.
(13) Mason, P. E.; Neilson, G. W.; Dempsey, C. E.; Barnes, A. C.; Cruickshank, J. M. *Proc. Natl. Acad. Sci. U.S.A.* **2003**, *100*, 4557–4561.
(14) Hribar, B.; Southall, N. T.; Vlachy, V.; Dill, K. A. *J. Am. Chem. Soc.* **2002**, *124*, 12302–12311.
(15) Rossky, P. J. *Proc. Natl. Acad. Sci. U.S.A.* **2008**, *105*, 16825–16826.
(16) Hua, L.; Zhou, R.; Thirumalai, D.; Berne, B. J. *Proc. Natl. Acad. Sci. U.S.A.* **2008**, *105*, 16928–16933.

Within this picture, questions arise concerning the nature of the interactions between denaturants and protein functional groups, especially those buried in the native state that are exposed upon unfolding. Since it has long been considered that hydrophobic interactions dominate the free energy of the native state,[17,18] denaturant interactions with exposed hydrophobic side chains that are buried in the native state are a compelling possibility. Classical measurements of amino acid transfer free energies into denaturant solution have characterized denaturant-mediated enhancement of the aqueous solubility of the hydrophobic amino acids.[19,20] In the past, these effects were ascribed to denaturant-induced alterations in the long-range structure of liquid water, although this has not been well-supported by experimental observations.[21−24] Alternatively, denaturant-mediated displacement of ordered waters from the hydrophobic surface via weak denaturant-surface interactions[25,26] provides a mechanism for attenuation of the hydrophobic effect that does not involve poorly characterized denaturant effects on long-range water structure.

It may still be questioned, however, whether interactions with the hydrophobic side chains of proteins make significant contributions to the activities of commonly used denaturants such as urea and guanidinium hydrochloride (GdmCl). Recent analyses have highlighted the important role for the peptide backbone in cosolute effects (both stabilizing and denaturing) on protein native state stability.[27] Urea, for example, has been shown to directly hydrogen bond to peptide backbone groups.[28] Further, a reanalysis of the energetics of urea-mediated enhancement of amino acid solubility indicates that the nonpolar side chains make small or even negative contributions to amino acid transfer into 1 M urea; only the aromatic amino acids and aliphatic leucine make positive contributions.[29] Also, several analyses of residual structure in urea or GdmCl-denatured proteins have identified clusters of hydrophobic side chains apparently resistant to the denaturant.[30−32] The ability of urea and Gdm^+ to uncoil helical polypeptides that lack significant stabilizing contributions from the hydrophobic effect,[33,34] and analyses of the interactions of these denaturants with unfolded polypeptide,[35] support contributions to the denaturant mechanism from denaturant-peptide backbone interactions.[28]

An interpretation that is consistent with much of the experimental data is that contributions from denaturant interactions with the polypeptide backbone are supplemented with effects arising from interaction with the aromatic side chains of proteins. This seems to be required at least for Gdm^+, since this denaturant is particularly effective in attenuating stabilizing indole−indole interactions between Trp side chains[34] and makes favorable cation−π interactions,[36] analogous to those observed between aromatic side chains and arginine in protein crystal structures.[37] The aromatic amino acids display the most favorable free energies for transfer from water into denaturant (urea and especially GdmCl),[19,20] consistent with early conclusions that interaction models for denaturant action should include the aromatic amino acids as well as the peptide backbone.[7]

The present study addresses the relative ability of GdmCl to attenuate stabilizing interactions involving hydrophobic "clusters" of aliphatic groups (in aqueous isopropanol) or aromatic groups (in aqueous pyridine), respectively. Small angle neutron scattering (SANS) experiments were used to monitor long-range clustering of these solutes, and the effects of GdmCl on that clustering, combined with MD simulations to analyze short-range structure, which allows a detailed interpretation of the molecular interactions between denaturant and nonpolar group. The observations support the conclusion that the effects of Gdm^+ on conformation-stabilizing interactions involving aromatic amino acid side chains are significant in the denaturing activity of GdmCl, while those involving interactions with the aliphatic side chains are less significant.

Methods

Experimental Procedures. Small-angle neutron scattering experiments were performed on the NG3 30 m SANS instrument at the National Institute of Standards and Technology Center for Neutron Research (NCNR) in Gaithersburg, MD. Solutions of pyridine and isopropanol at 3 *m* concentration in D_2O were prepared by the direct addition of the solute to a known amount of heavy water (about 5 g). Three molal solutions of GdmCl were made by adding exact amounts of D_2O (typically 5 g) to known amounts of GdmCl. Solutions containing 3 *m* GdmCl and 3 *m* of either pyridine or isopropanol were made by first preparing a 3 *m* solution of GdmCl (about 5 g), then adding the appropriate amount of either isopropanol or pyridine. To remove dust the solutions were filtered through surfactant-free cellulose acetate filters (Nalgene) of 0.2 μm pore size. Neutrons of wavelength $\lambda = 6$ Å with a distribution ($\Delta\lambda/\lambda$) of 15% were incident on samples held in 5 mm path length quartz cells. The sample-to-detector distance was chosen to give an overall q-range of $0.014\ \text{Å}^{-1} < q < 0.44\ \text{Å}^{-1}$, where $q = (4\pi/\lambda)\sin(\theta/2)$ is the magnitude of the scattering vector. Sample scattering was corrected for background and empty cell scattering, and the sensitivities of individual detector pixels were normalized with respect to the isotropic scattering of plexiglass. The corrected data sets were circularly averaged and placed on an absolute scale of cm^{-1} using direct beam transmission measurements. Data was modeled using nonlinear least-squares with software freely available from the NCNR.[38]

Computational Procedures. Molecular dynamics simulations were performed for four different solutions: a 3 *m* solution of

(17) Kauzmann, W. *Adv. Protein Chem.* **1959**, *14*, 1–63.
(18) Dill, K. A. *Biochemistry* **1990**, *29*, 7133–7155.
(19) Nozaki, Y.; Tanford, C. *J. Biol. Chem.* **1963**, *238*, 4074–4081.
(20) Nozaki, Y.; Tanford, C. *J. Biol. Chem.* **1970**, *245*, 1648–1652.
(21) Sharp, K. A.; Madan, B.; Manas, E.; Vanderkooi, J. M. *J. Chem. Phys.* **2001**, *114*, 1791–1796.
(22) Batchelor, J. D.; Olteanu, A.; Tripathy, A.; Pielak, G. J. *J. Am. Chem. Soc.* **2004**, *126*, 1958–1961.
(23) Rezus, Y. L. A.; Bakker, H. J. *Proc. Natl. Acad. Sci. U.S.A.* **2006**, *103*, 18417–18420.
(24) Soper, A. K.; Castner, E. W.; Luzar, A. *Biophys. Chem.* **2003**, *105*, 649–666.
(25) Kuharski, R. A.; Rossky, P. J. *J. Am. Chem. Soc.* **1984**, *106*, 5794–5800.
(26) Muller, N. *J. Phys. Chem.* **1990**, *94*, 3856–3859.
(27) Auton, M.; Bolen, D. W. *Proc. Natl. Acad. Sci. U.S.A.* **2005**, *102*, 15065–15068.
(28) Lim, W. K.; Rösgen, J.; Englander, S. W. *Proc. Natl. Acad. Sci. U.S.A.* **2009**, *106*, 2595–2600.
(29) Auton, M.; Holthauzen, L. M. F.; Bolen, D. W. *Proc. Natl. Acad. Sci. U.S.A.* **2007**, *104*, 15317–15322.
(30) Neri, D.; Billeter, M.; Wider, G.; Wüthrich, K. *Science* **1992**, *257*, 1559–1563.
(31) Shortle, D.; Ackerman, M. S. *Science* **2001**, *293*, 487–489.
(32) Chugh, J.; Sharma, S.; Hosur, R. V. *Biochemistry* **2007**, *46*, 11819–11832.
(33) Scholtz, J. M.; Barrick, D.; York, E. J.; Stewart, J. M.; Baldwin, R. L. *Proc. Natl. Acad. Sci. U.S.A.* **1995**, *92*, 185–189.
(34) Dempsey, C. E.; Piggot, T. J.; Mason, P. E. *Biochemistry* **2005**, *44*, 775–781.
(35) Moglich, A.; Krieger, F.; Kiefhaber, T. *J. Mol. Biol.* **2005**, *345*, 153–162.
(36) Mason, P. E.; Brady, J. W.; Neilson, G. W.; Dempsey, C. E. *Biophys. J.* **2007**, *93*, L04–L06.
(37) Flocco, M. M.; Mowbray, S. L. *J. Mol. Biol.* **1994**, *235*, 709–717.
(38) Kline, S. R. *J. Appl. Crystallogr.* **2006**, *39*, 895–900.

pyridine in water; a 3 *m* solution of isopropanol in water; a mixed solution of 3 *m* pyridine and 3 *m* guanidinium chloride in water; and a mixed solution of 3 *m* isopropanol and 3 *m* guanidinium chloride in water. Identical procedures were used for all four simulations. The method will only be described in detail for the setup of the pyridine/GdmCl simulation. The starting coordinates for this mixed solution were generated by randomly placing 36 Gdm^+ ions, 36 Cl^- ions and 36 pyridine molecules in a cubic box of length 34 Å with random orientations and no van der Waals overlaps. This box was superimposed on a 34 Å box of 1296 previously equilibrated TIP3P water molecules,[39] and all those water molecules that produced van der Waals clashes were removed. Additional water molecules were then randomly deleted to produce the correct concentration, with 667 remaining water molecules. This side of this box was then rescaled to 30.6312 Å to give the correct number density of 0.0972 atoms $Å^{-3}$. For the 3 *m* solution of pyridine in water, there were 56 pyridine molecules and 1036 water molecules (3.003 *m*), with a box size of 33.6771 Å and a number density of 0.0975 atoms $Å^{-3}$. For the 3 *m* isopropanol solution in water, there were 56 isopropanol molecules and 1036 water molecules (also 3.003 *m*) with a box size of 33.4606 Å and a number density of 0.1009 atoms $Å^{-3}$. For the mixed solution of 3 *m* isopropanol and 3 *m* guanidinium chloride in water, there were 36 molecules each of isopropanol, guanidinum ions, and chloride ions in 667 water molecules, for a concentration of 2.999 *m* for all species, with a box size of 30.4602 Å and a number density of 0.1001 atoms $Å^{-3}$.

The simulations employed a guanidinium potential energy function based on the parameters for arginine in the CHARMM22 protein force field,[40] with the atomic partial charges assigned symmetrically (atom charges: C 0.64; N −0.80; H 0.46). Water molecules were represented using the TIP3P model[41] and the pyridine and isopropanol parameters were taken from the CHARMM small molecule force field.[39] All simulations were performed using the CHARMM program,[42,43] with chemical bonds to hydrogen atoms kept fixed using SHAKE[44] and with a time step of 1 fs.

All van der Waals interactions were smoothly truncated on an atom-by-atom basis using switching functions between 10.5 and 11.5 Å,[17] while electrostatic interactions were treated using the Ewald method,[45] with a real space cutoff of 12.5 Å, $\kappa = 0.333$ and a K_{max}^2 of 27. Initial velocities were assigned from a Boltzmann distribution (300 K) followed by 5 ps of equilibration dynamics during which velocities were reassigned every 0.1 ps. The simulations were then each run for 10.0 ns with no further velocity reassignment. The first 3.0 ns of each simulation was taken as equilibration, and the remaining 7.0 ns was used for analysis.

Table 1. Results of Fitting SANS Data to Ornstein−Zernicke Model of Concentration Fluctuations

sample	$I(0)$ (cm^{-1})	ξ (Å)	b (cm^{-1})	$\sqrt{\chi^2/N}$[a]
3 *m* isopropanol	0.071 ± 0.011	1.40 ± 0.15	0.22 ± 0.011	0.93
3 *m* isopropanol + 3 *m* GdmCl	0.070 ± 0.013	1.44 ± 0.19	0.32 ± 0.013	1.00
3 *m* pyridine	0.234 ± 0.0004	4.53 ± 0.017	0.14 ± 0.0004	1.10
3 *m* pyridine + 3 *m* GdmCl	0.089 ± 0.0014	2.72 ± 0.054	0.24 ± 0.0016	0.84

[a] $\sqrt{\chi^2/N}$ is the reduced chi-squared, $N = 120$ is the number of fitted data points.

Results and Discussion

SANS Data and Analysis. Coherent scattering in SANS arises from the presence of distinct regions in a sample that have different (coherent) scattering length densities. In these solutions, clustering of the solute provides the structure, while the use of a deuterated solvent (D_2O) versus hydrogenated solutes provides the coherent scattering contrast. If there is no clustering (i.e., a uniform solution with no concentration fluctuations), there is no coherent scattering. Likewise, if the coherent scattering length density of a cluster is not different from its surrounding solvent, there is no coherent SANS signal. For these samples the SANS data sets were modeled using the Ornstein−Zernike equation for concentration fluctuations:

$$I(Q) = \frac{I(0)}{1 + Q^2\xi^2} + b \qquad (1)$$

where $I(0)$ is the intensity at $Q = 0$, ξ is the correlation length of the density fluctuations, and b is the incoherent background arising from the incoherent cross section of the sample (dominated by hydrogen). The radius of the cluster is related to the correlation length as $r_{cluster} = \sqrt{5}\xi$. Data were fitted using nonlinear optimization, and all three fitted parameters are shown in Table 1. All model fits are excellent, with a reduced χ-squared near one.

It is clear from the shape of the SANS curves shown in Figure 1 that D_2O and 3 *m* GdmCl in D_2O show no coherent structure; that is, they are uniform solutions on the molecular level within the resolution of SANS. Both the solutions of pyridine in D_2O (Figure 1a) and of isopropanol in D_2O (Figure 1b) show a coherent structure, with larger correlation lengths present in pyridine solutions, corresponding to clusters of tens to hundreds of molecules, while the small correlation length for the isopropanol implies aggregates of only a few molecules, as would be expected. The presence of structure in these solutions is consistent with previous SANS experiments.[46−48] When 3 *m* GdmCl is added to isopropanol (Figure 1b), there is no change in the correlation length or $I(Q = 0)$ scattering, indicating no change in its clustering behavior. The only change is an increase in the incoherent scattering, which is expected from the addition of hydrogenated GdmCl. On the other hand, adding 3 *m* GdmCl to the pyridine solution (Figure 1a) significantly decreases the size of structures in the solution, quantified as a decrease in the

(39) MacKerell, A. D.; Bashford, D.; Bellott, M.; Dunbrack, R. L.; Evanseck, J. D.; Field, M. J.; Fischer, S.; Gao, J.; Guo, H.; Ha, S.; Joseph-McCarthy, D.; Kuchnir, L.; Kuczera, K.; Lau, F. T. K.; Mattos, C.; Michnick, S.; Ngo, T.; Nguyen, D. T.; Prodhom, B.; Reiher, W. E.; Roux, B.; Schlenkrich, M.; Smith, J. C.; Stote, R.; Straub, J.; Watanabe, M.; Wiorkiewicz-Kuczera, J.; Yin, D.; Karplus, M. *J. Phys. Chem. B* **1998**, *102*, 3586–3616.
(40) Mason, P. E.; Dempsey, C. E.; Neilson, G. W.; Brady, J. W. *J. Phys. Chem. B* **2005**, *109*, 24185–24196.
(41) Jorgensen, W. L.; Chandrasekhar, J.; Madura, J. D.; Impey, R. W.; Klein, M. L. *J. Chem. Phys.* **1983**, *79*, 926–935.
(42) Brooks, B. R.; Bruccoleri, R. E.; Olafson, B. D.; Swaminathan, S.; Karplus, M. *J. Comput. Chem.* **1983**, *4*, 187–217.
(43) Brooks, B. R.; Brooks, C. L., III; MacKerell, A. D., Jr.; Nilsson, I. L.; Petrella, R. J.; Roux, B.; Won, Y.; Archontis, G.; Bartels, C.; Boresch, S.; Caflisch, A.; Caves, L.; Cui, Q.; Dinner, A. R.; Feig, M.; FischerI, S.; Gao, J.; Hodoscek, M.; Im, W.; Kuczera, K.; Lazaridis, T.; Ma, J.; Ovchinnikov, V.; Paci, E.; Pastor, R. W.; Post, C. B.; Pu, J. Z.; Schaefer, M.; Tidor, B.; Venable, R. M.; Woodcock, H. L.; Wu, X.; Yang, W.; York, D. M.; Karplus, M. *J. Comput. Chem.* **2009**, *30*, 1545–1614.
(44) van Gunsteren, W. F.; Berendsen, H. J. C. *Mol. Phys.* **1977**, *34*, 1311–1327.
(45) Darden, T.; York, D.; Pedersen, L. *J. Chem. Phys.* **1993**, *98*, 10089–10092.
(46) D'Arrigo, G.; Teixeira, J. *J. Chem. Soc. Faraday Trans.* **1990**, *86*, 1503–1509.
(47) Almásy, L.; Jancsó, G. *J. Mol. Biol.* **2004**, *113*, 61–66.
(48) Bako, I.; Palinkas, G.; Dore, J. C.; Fischer, H.; Jovari, P. *Chem. Phys. Lett.* **2004**, *388*, 468–472.

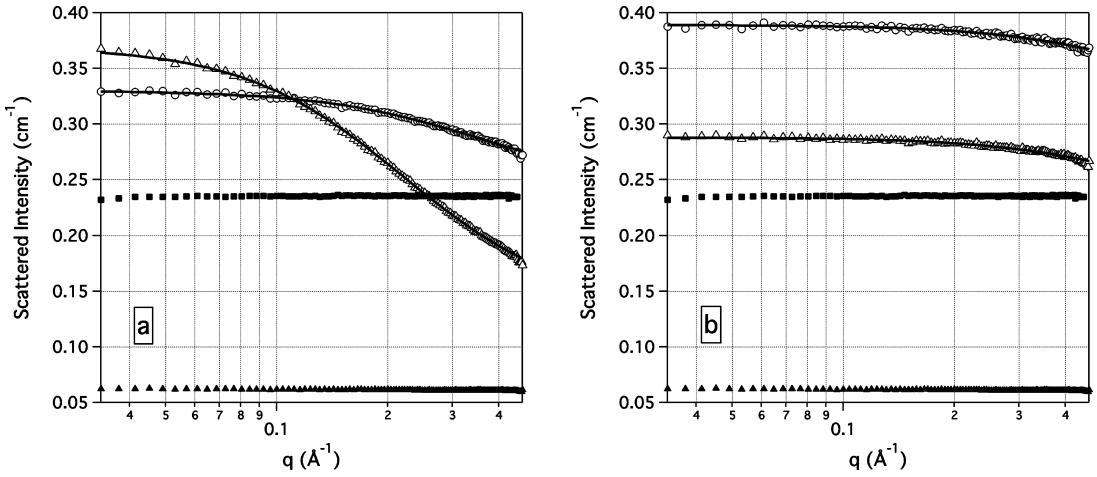

Figure 1. SANS data from: (a) 3 *m* pyridine in D_2O (△), 3 *m* pyridine plus 3 *m* GdmCl in D_2O (○); and (b) 3 *m* isopropanol in D_2O (△), 3 *m* isopropanol plus 3 *m* GdmCl in D_2O (○). Solid lines are model fits using the O-Z model. The addition of 3 *m* GdmCl to pyridine clearly reduces the length scale of the aggregates, while GdmCl has no effect on the aggregates of isopropanol. The structureless scattering from D_2O (solid triangles), and 3 *m* GdmCl in D_2O (solid squares) are shown in each graph for comparison. Both graphs are on the same scale and are in absolute units. The height of the symbols is representative of one standard deviation of the measured intensity.

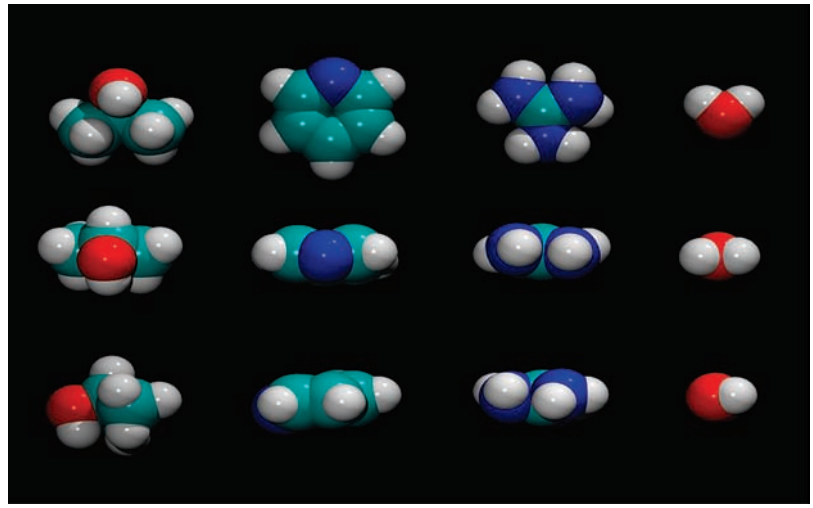

Figure 2. Size and shape of the species used in this study. Shown on the left is isopropanol; on the middle left is the flat pyridine molecule. On the middle right is the flat denaturant guanidinium ion, and on the right is water, providing a visual reference of the comparative sizes. The top, middle and bottom rows show different orientations of these molecules. The molecular volumes of these molecules are 71, 78, 57, and 19 Å^3 for isopropanol, pyridine, Gdm^+, and water, respectively.

correlation length from 4.53 to 2.72 Å and a similar decrease in the $I(Q = 0)$ scattering.

Although both isopropanol and pyridine are soluble in water, they have extensive hydrophobic regions (see Figure 2) and might be expected to aggregate in aqueous solution to minimize solvent-exposed surface. Such aggregation has previously been reported for methanol in water using neutron diffraction, although in this case the small hydrophobic surface of the methyl groups does not permit the development of large-scale aggregates.[49] Stacking aggregation of guanidinium ions has also been observed in MD simulations.[40] Isopropanol, with its more spherical hydrophobic surface, shows less propensity to aggregate than the flat pyridine molecule, and those aggregates of isopropanol that are present show less propensity to dissociate in the presence of guanidinium than is the case for pyridine aggregates. The isopropanol clusters are essentially insensitive to the presence of GdmCl, while the pyridine clusters are significantly disrupted by the denaturant.

The scattering intensity $I(Q = 0)$ is sensitive to both the composition and concentration (number density) of the clusters. For this reason, it is not possible to determine simultaneously the exact composition of the clusters and the concentration of the clusters. This has been described previously by D'Arrigo and Teixeira,[46] who showed that micelle-like clusters of solute in D_2O or water-solute aggregates in the remaining water and solute monomers are the two most likely structures present in solution.

MD Simulations and Analysis. The SANS data do not contain sufficient resolution for characterization on the molecular scale of the interactions underlying solute aggregation in the isopropanol and pyridine solutions, or the disaggregation of pyridine by GdmCl. MD simulations allow detailed characterization of molecular interactions in these solutions without necessarily being expected to reproduce the features of the SANS data

(49) Mason, P. E.; Neilson, G. W.; Enderby, J. E.; Saboungi, M.-L.; Dempsey, C. E.; MacKerell, A. D.; Brady, J. W. *J. Am. Chem. Soc.* **2004**, *126*, 11462–11470.

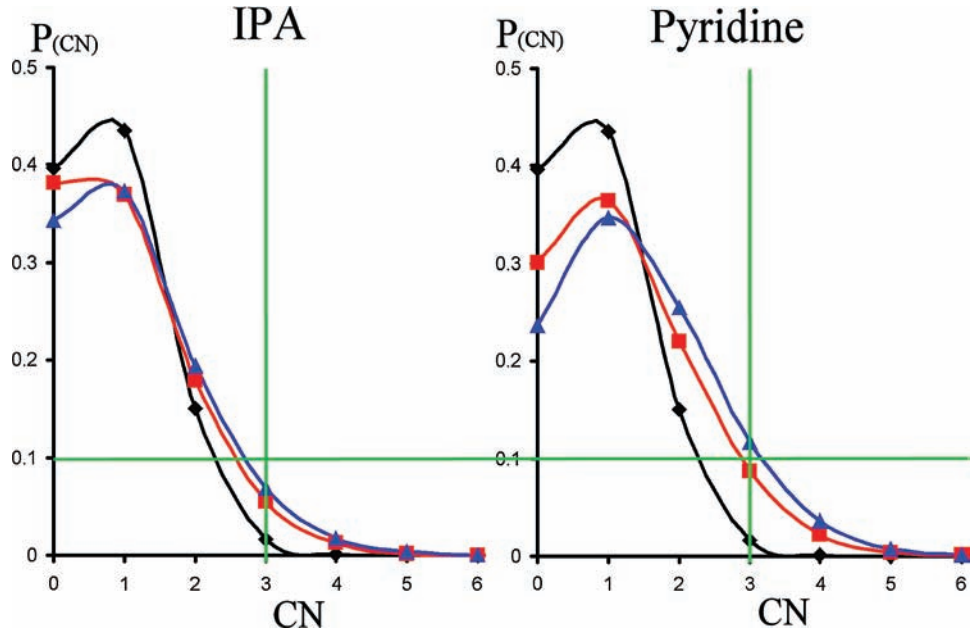

Figure 3. Probability of finding solute−solute coordination numbers for 3 *m* isopropanol (left, blue), 3 *m* isopropanol in 3 *m* GdmCl (left, red), 3 *m* pyridine (right, blue), and 3 *m* pyridine in 3 *m* GdmCl (red), as calculated from MD simulations. Shown in black in each panel is the solute−solute CN for Gdm^+ in a 3 *m* solution of GdmCl, a species known to show mild homoion association in a specific stacking type orientation that does not result in significant longer range structures.[49]

characteristic of long-range structure. Insight into the different aggregation properties of isopropanol and pyridine in aqueous solution should be manifest in a reliable simulation. Accordingly, MD simulations were designed to reproduce the experimental solutions studied by SANS (3 *m* pyridine; 3 *m* pyridine with 3 *m* GdmCl; 3 *m* isoproponal; 3 *m* propanol with 3 *m* GdmCl; see Methods) and were analyzed with respect to their associative behaviors.

The size and topology of large-scale aggregates of the solutes are reflected in the solute−solute coordination number (CN). As the CN increases above 1, the solute can form extended aggregates or clusters. In the present simulations, two solute molecules were taken to be coordinated if any of their heavy atoms were within 4.5 Å of one another. A CN of 0 is a free solute, a CN of 1 indicates either a dimer or the termination of a cluster, a CN of 2 is part of a chain, and a CN of 3 or higher represents the branch points of a three-dimensional cluster or network. The probabilities of finding each coordination number in the different solutions are shown in Figure 3. The simplest measure of the association of the solute is the probability of finding a free solute molecule. There is more free isopropanol in the 3 *m* solution of isopropanol (∼38% free isopropanol, 62% not free) than there is free pyridine in the 3 *m* pyridine solution (∼27% free pyridine, 73% not free), showing that there is more solute−solute association in the pyridine solution. This association may be compared to the previously observed association of Gdm^+ ions (in GdmCl), which displays weak face-to-face stacking,[40] occasionally forming longer stacks (Figure 3). Rarely do these stacks exceed four monomers in size, so they do not reach nanometer-scale dimensions. In such stacks, the coordination number for the guanidinium ions in the interior of the stack is 2. Consistent with the SANS measurement (Figure 1), there is more free Gdm^+ in the solution containing only GdmCl than free pyridine in the pyridine solution, or free isopropanol in the isopropanol solution. There is also a significantly lower number of highly aggregated molecules (the probability of finding a solute with CN 3 or higher) of 1.7% for the Gdm^+ solution, compared to 8.9% for the isopropanol solution, and 16% for the pyridine solution (Figure 3). For isopropanol and isopropanol with GdmCl there is about 34 and 35% free hydrophobic solute, respectively, while in the pyridine solutions this contrast is significantly increased to 23 and 30%. This observation shows that the association of isopropanol is essentially insensitive to the presence of denaturant, while the association of pyridine displays a significant dispersion by GdmCl. Consistent with the CN data of Figure 3 and with the SANS data of Figure 1, analysis of cluster size in the MD simulations demonstrates a shift to smaller pyridine clusters in the presence of GdmCl and the absence of an effect of GdmCl on isopropanol cluster size (Figure 4).

An alternative way of highlighting the effects of GdmCl on these hydrophobic solutes involves examining the number of solute and solvent atoms within a 4.5 Å cutoff around the solute (Tables 2 and 3). Consistent with the SANS results, the addition of GdmCl to isopropanol solution does not significantly change the number of isopropanol atoms within 4.5 Å of the isopropanol molecules, while there is about a 10% decrease in the number of pyridine atoms around pyridine after the addition of GdmCl. The average solute−solute coordination number (SSCN) was also calculated, where any two solute molecules with any of their heavy atoms within 4.5 Å of each other are classified as being in contact. Again it was found that there is a higher degree of association in the pyridine-water system than in the isopropanol−water system (SSCNs of 1.03 versus 0.76), while the addition of GdmCl has a lesser effect on the isopropanol−water system (SSCNs of 0.68 and 0.76 for isopropanol both with and without GdmCl, respectively), compared to the addition of GdmCl to the pyridine solution (SSCN of 1.03 and 0.92 for pyridine with and without GdmCl). This reflects the higher association of pyridine over isopropanol, and the much higher sensitivity of pyridine clusters to GdmCl. These observations are entirely consistent with the effects of GdmCl on solute cluster size in the SANS experiments (Figure 1).

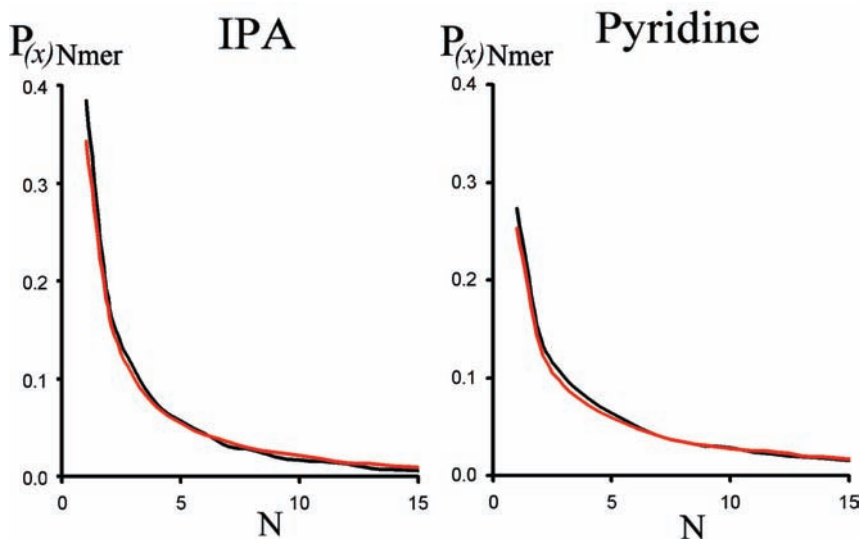

Figure 4. (Left) Probability of a solute being found in a cluster of size N in isopropanol solution (gray), and in an isopropanol/GdmCl solution (black). (Right) Probability of a solute being found in a cluster of size N in pyridine solution (gray) and in a pyridine/GdmCl solution (black).

Table 2. Atomic CN for Each Type of Nuclei in the 3 *m* Isopropanol and 3 *m* Isopropanol with GdmCl Simulations[a]

	CN IPA solution	CN IPA/Gdm solution	ratio
C1−3	2.45	2.22	0.91
O2	0.58	0.49	0.85
HO2	0.65	0.53	0.82
H_{non}	5.19	4.71	0.91
Ow	15.19	12.83	0.84
Hw	29.19	24.34	0.83
C_{Gdm}	0.00	0.72	
N_{Gdm}	0.00	1.99	
H_{Gdm}	0.00	3.80	
Cl	0.00	0.42	

[a] Nuclei types are C1-3 (carbon on isopropanol), O2, oxygen on isopropanol, HO2, hydroxyl hydrogen on isopropanol, H_{non}, non-exchangeable hydrogens on isopropanol; Ow and Hw, the water nuclei; C_{Gdm}, N_{Gdm}, H_{Gdm}, and Cl the GdmCl nuclei.

Table 3. Atomic CN for Each Type of Nuclei in the 3 *m* Pyridine and 3 *m* Pyridine with GdmCl Simulations[a]

	CN pyridine solution	CN pyridine/GdmCl solution	ratio
C1−5	5.25	4.70	0.89
NZ	0.93	0.85	0.91
H_{non}	5.13	4.53	0.88
Ow	15.82	14.04	0.89
Hw	30.33	26.47	0.87
C_{Gdm}	0.00	0.78	
N_{Gdm}	0.00	2.18	
H_{Gdm}	11.31	4.17	
Cl	0.00	0.46	

[a] Nuclei types are C1-5 (carbon on pyridine), NZ, nitrogen on pyridine, H_{non}, non-exchangeable hydrogens on pyridine, Ow and Hw, the water nuclei, C_{Gdm}, N_{Gdm}, H_{Gdm}, and Cl the GdmCl nuclei.

The molecular interactions underlying the solute coordination properties, and the attenuation by Gdm^+ of pyridine clustering, can be assessed by calculating specific atom number densities around the solutes. These data are shown in Figures 5−7. The densities of H_{PY} and C_{PY} around pyridine in the 3 *m* MD simulation indicates that pyridines preferentially associate in a T-type geometry (Figures 5 and 6), since the H_{PY} forms a cloud on the inside (closer to the pyridine) of the C_{PY} cloud; in a stacking type interaction the C_{PY} and H_{PY} should be coincident. Conversely, in the simulation of pyridine in GdmCl, the density maps show that the Gdm^+ ions preferentially stack in a parallel fashion to the pyridine solute, since the H_{Gdm} and N_{Gdm} clouds are coincident. These geometries are apparent in snapshots from the simulation (Figure 6), and the planar stacking arrangement is similar to the planar homoion stacking that Gdm^+ ions display in GdmCl solution. An exception occurs when the Gdm^+ makes a hydrogen bond to the nitrogen of the pyridine, where the H_{Gdm} comes on the inside of the N_{Gdm} cloud, as observed in the higher contour plots on the bottom row of Figure 5.

In Figure 7, the densities of C_{IPA} around isopropanol are shown both from the simulations without GdmCl and in the presence of the denaturant. The isopropanol−isopropanol interaction is essentially unaffected by the presence of Gdm^+, and the density of isopropanol around isopropanol is not significantly diminished by Gdm^+. The density map suggest that the preferred mechanism of association between two isopropanol molecules is by the contact of the methyl groups, although this preference is not as strong as those found in pyridine-pyridine association. The preferred mode of interaction of Gdm^+ with isopropanol is by hydrogen bonding to hydroxyl group, and interaction of Gdm^+ with the nonpolar (methyl) groups of isopropanol is weak. The displacement of water molecules hydrogen bonding to the isopropanol hydroxyl group by Gdm^+ dominates the reduction of the water CN in isopropanol−GdmCl mixtures compared to denaturant-free solution (Table 2).

The qualitative agreement between the experimental and simulation results in these studies supports the general interpretation of the data provided by the simulations. Clearly, however, the quantitative results reported from the calculations will depend on the details of the force fields and water models employed, particularly, for example, in determining the strength of water-solute interactions. The TIP3P water model used here, for example, is known to be somewhat less tetrahedrally structured than real water.[50] However, the guanidinium parameters have been used successfully with this water model before,[49] and the geometric character of many of the interactions suggests a weak dependence of the results on force field details. Thus,

(50) Mason, P. E.; Brady, J. W. *J. Phys. Chem. B* **2007**, *111*, 5669–5679.

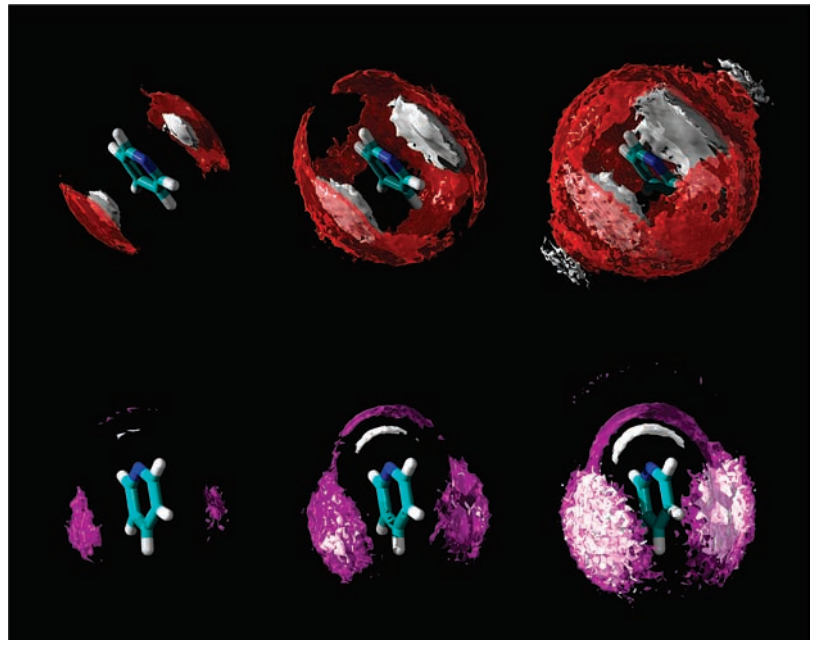

Figure 5. (Upper) Density maps of H_{PY} (white) and C_{PY} (red) for pyridine around pyridine in the GdmCl-free simulation. From left to right the contours denote number densities of 0.0250, 0.0175, and 0.0135 atoms $Å^{-3}$. These density maps indicate that T-type pyridine-pyridine interactions are preferred (see Figure 7). (Lower) Density maps [H_{Gdm} (white), N_{Gdm} (purple)], for Gdm^+ around pyridine. From left to right the N_{Gdm} have contours are 0.0150, 0.0105, 0.0081 atoms $Å^{-3}$ while the H_{Gdm} contours have contours of double these values. This indicates that the Gdm^+ ions tend to stack face-on to the pyridine, except when they hydrogen bond to the nitrogen of the pyridine, yielding a "headphones" shaped density map.

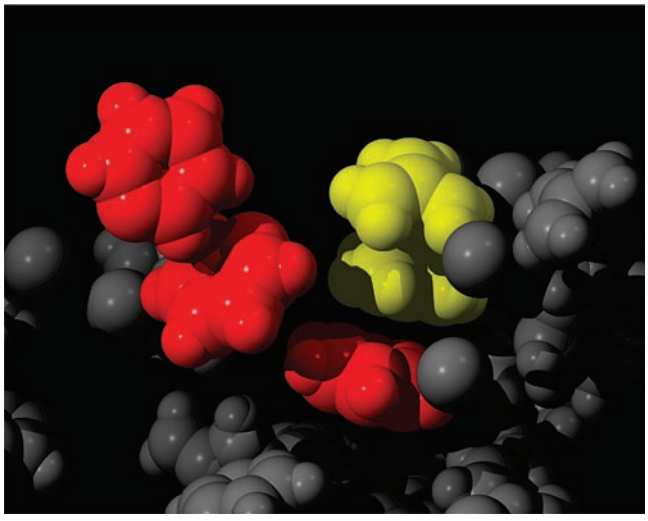

Figure 6. Snapshot from the pyridine−GdmCl simulation, showing typical solute−solute interactions. The two left most pyridines (red) are showing a T-type interaction while the two Gdm^+ ions (yellow) and one pyridine on the right are making stacking interactions.

the qualitative picture provided by the simulations is unlikely to be strongly dependent on the parametrization.

Conclusions

The SANS and MD data show that both isopropanol and pyridine undergo measurable aggregation in aqueous solution, consistent with weak nonpolar interactions driven by the hydrophobic effect (supplemented with an electrostatic contribution in the case of the pyridine-pyridine association as indicated by the T-type ring interactions). These solutions provide a means of assessing group-specific effects of GdmCl by measuring the ability of the denaturant to dissociate aggregates dominated either by aromatic interactions (pyridine as an analog of the aromatic side chains of proteins), or "lumpy" aliphatic groups (the aliphatic moiety of isopropanol is equivalent to the side chain of valine). The data support the conclusion that Gdm^+ does not make favorable interactions with "lumpy" aliphatic groups such as that of isopropanol. The lack of dissociation of isopropanol clustering by GdmCl also demonstrates that any putative generalized effects of Gdm^+ on "water structure" is ineffective in promoting dispersal of these hydrophobic groups in water. These observations indicate that the enhancement, by Gdm^+, of the aqueous solubility of the aliphatic groups buried in the native state structures of proteins may make minimal contributions to the denaturant activity of Gdm^+.

On the other hand Gdm^+ ions interact with the planar aromatic faces of pyridine, displacing water molecules from these hydrophobic surfaces, and are thus effective in dissociating the "hydrophobic" clustering of pyridine in water. This model is consistent with previous observations that Gdm^+ is a strong denaturant of structure stabilized by indole−indole interactions involving the planar aromatic side chain of tryptophan.[34] In this case, it can be generalized that enhancement of the aqueous solubility of the aromatic side chains of proteins makes a significant contribution to the denaturant activity of Gdm^+.

These observations highlight the importance of complementarity, in geometry and hydration properties,[34,36,51−53] in solute−solute (or solute−side chain) interactions in aqueous solution. Poorly hydrated solute (or protein) moieties can associate with the displacement of weakly associated waters from their interacting surfaces. However, the interacting surfaces must be "matched" to maximize van der Waals contacts and minimize voids. These considerations underlie

(51) Dempsey, C. E.; Mason, P. E. *J. Am. Chem. Soc.* **2006**, *128*, 2762–2763.
(52) Dempsey, C. E.; Mason, P. E.; Brady, J. W.; Neilson, G. W. *J. Am. Chem. Soc.* **2007**, *129*, 15895–15902.
(53) Chandler, D. *Nature* **2005**, *437*, 640–647.

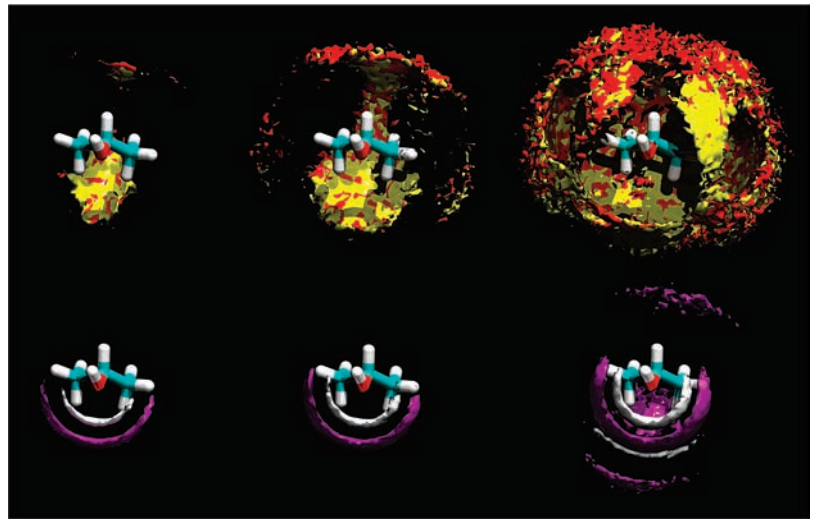

Figure 7. (Upper) Density map for C_{IPA} around isopropanol in the simulation without GdmCl (red), and with GdmCl (yellow). From left to right the density contours have values of 0.015, 0.012. 0.0088 atoms Å^{-3}. (Lower) Density map for N_{Gdm} (purple) and H_{Gdm} (white) around isopropanol (contours at 0.015, 0.012, and 0.0088 atoms Å^{-3}, left to right, for N_{Gdm}, and at twice these values for H_{Gdm}). The dominant interaction seen between Gdm^+ and isopropanol is the hydrogen bond with the hydroxyl oxygen of the isopropanol.

the observations that the hydrophobic effect, and its disruption by denaturants, has a marked size dependence, with small aliphatic groups like methane (and the side chain of alanine) exhibiting positive transfer free energies from aqueous solution into denaturant solution, for example.[38] The recent reappraisal of transfer free energies for amino acid side chains from water into urea solution[29] indicates that these considerations may apply more generally to the commonly used small planar denaturants, since the transfer of all of the aliphatic amino acid side chains except Leu into 1 M urea is unfavorable. Thus, even though the aliphatic groups of the amino acids Val, Leu, and Ile are considerably larger than methane/methyl, their surface is poorly matched to the planar denaturant molecule, limiting productive displacement of weakly associating waters from the aliphatic side chain surfaces by the denaturant. The interaction of the Gdm^+ cation with aromatic side chains is particularly favorable due to the cation$-\pi$ nature of the interaction.[34,37,52] MD simulations also indicate that cation$-\pi$ interactions can be made with the delocalized π-systems of the side chain amide groups of Gln and Asn, and especially with the guanidine side chain of Arg,[36] although in simulations this may reflect complementary planarity since molecular orbitals are not explicitly modeled but are only implicitly represented by force field parametrization. Interactions of these groups (aromatic and planar π-systems) with urea is likely to be less favorable (urea, for example, is a much weaker denaturant of structure stabilized by indole$-$indole interactions compared to Gdm^+).[34] The specific and favorable interactions of Gdm^+ with weakly hydrated π-systems, particularly the aromatic amino acid side chains, are likely to contribute to the enhanced denaturant activity of GdmCl over urea, over and above any differences in the effectiveness of these denaturing solutes in "solubilizing" the peptide backbone via hydrogen bond interactions[34,35] which recent evidence supports as the dominant mechanism for the denaturant activity of these molecules.

Acknowledgment. This project was supported by grant GM63018 from the National Institutes of Health. The work utilized facilities supported in part by the National Science Foundation under Agreement DMR-0454672. The mention of commercial products does not imply endorsement by NIST, nor does it imply that the materials or equipment identified are necessarily the best available for the purpose.

JA903478S